

Supporting Information

Membrane lipids are an integral part of transmembrane allosteric sites in GPCRs: A case study of cannabinoid CB1 receptor bound to a negative allosteric modulator, ORG27569, and analogs

Peter Obi and Senthil Natesan*

College of Pharmacy and Pharmaceutical Sciences, Washington State University, Spokane, WA 99202, USA

Email ID: senthil.natesan@wsu.edu

Contents

Table S1. Structural and physicochemical properties of ORG27569 and CC55940.....	2
Table S2. The experimental binding affinity and cooperativity data.....	3
Table S3. Characteristics of the orthosteric and allosteric binding sites of CB1R.....	3
Table S4. Lipid compositions of the asymmetric bilayer used in the simulations.....	4
Table S5. The total, nonpolar, and polar BSA and MESA.....	5
Table S6. The binding free energies of various CB1R ligands were calculated using the MMPBSA method considering explicit membrane lipids	6
Table S7. The per-lipid binding free energy contribution by several lipids for various CB1R ligands, calculated using the MMPBSA method considering explicit membrane lipids.	7
Table S8. The percentage contact occupancy (%) of the studied ligands with various functional groups of the bilayer lipids.....	8
Table S9. The binding free energies of various CB1R ligands were calculated using the MMPBSA method, considering implicit heterogeneous membrane regions represented by distinct dielectric constants.....	9
Table S10. The amino acid details for the Cholesterol Consensus Motif (CCM) in GPCRs....	10
Fig. S1. The internal angle of ORG27569.....	11
Fig. S2. Binding of ORG27569 during the WT-metaD simulation leads to the rearrangement of lipids around the binding site.. ..	12
Fig. S3. ORG27569 remains stable at the binding site during the entire 1 microsecond long unbiased MD simulation.. ..	13
Fig. S5. The binding orientations of ORG7569 and analogs.. ..	15
Fig. S6. Schematic representation of the CB1R-ligand complex is directly in contact with the membrane lipids.....	16

Fig. S7. The number of lipid molecules directly in contact with the bound ligands..17

Fig. S8. The effect of ORG27569 and its various analogs on H-bond distances and other molecular interactions of the agonist, CC55940, at the orthosteric site..18

Fig. S9. Multiple sequence alignment of residues that were involved in the access process of ORG17569 to the transmembrane allosteric site of CB1 receptor.....19

Fig. S10. Multiple sequence alignment of residues at the transmembrane allosteric binding site of CB1 receptor.....20

Fig. S11. Lipid species that were directly in contact with Compound 21.21

Fig. S12. Lipid species that were directly in contact with ICAM-b.....21

Fig. S13. Lipid species that were directly in contact with Compound 13.22

Fig. S14. Lipid species that were directly in contact with Compound 11j.....22

Fig. S15. Lipid species that were directly in contact with Compound 12f.23

Table S1. Structural and physicochemical properties of ORG27569 (a negative allosteric modulator) and CC55940 (an orthosteric agonist).

property	ORG27569	CC55940
Molecular weight	409.9	376.6
ClogP*	5.89	5.87
HB donor count	2	3
HB acceptor count	2	3
rotatable bond count	6	10
TPSA (Å ²)	48.1	60.7
heavy atom count	29	27

*log *P* values were calculated using Biolum¹.

Table S2. The experimental binding affinity and cooperativity data for the studied ligands.

Compound	K_B (nM) ^{2-4,*}	α ²⁻⁴	EC_{50} (μ M) ⁵	BS (%)
ORG27569	217.3 (170.3 – 277.2)	6.95	0.14	243.8
ICAM-b	469.9 (126.2 – 1750)	17.60		
Compound 13	207.4 (155.9 – 2759)	19.68	0.05	226.8
Compound 11j	167.3 (23.39 – 1197)	16.55		
Compound 12f	89.1 (47.08 – 168.4)	5.1		
Compound 21	NA	NA	0.09	206.7

K_B – equilibrium dissociation constant ($n = 2$), which reflects the binding affinity of the ligands to the allosteric site; α – binding cooperativity factor for the tested allosteric modulators using [³H]CP55940 as the orthosteric ligand. When $\alpha = 1.0$, the test modulator does not alter orthosteric ligand binding. If $\alpha > 1.0$, the test modulator increases orthosteric ligand binding (positive allosteric modulation of orthosteric ligand binding). *Data are presented as the mean with the corresponding 95% confidence limits from at least three independent experiments.

EC_{50} values ($n = 2$) represent the enhancement or inhibition of radioligand binding by increasing compound concentrations; BS: % of binding stimulation at the maximum concentration tested (10 μ M)

Table S3. Characteristics of the orthosteric and allosteric binding sites of CB1R, calculated using fpocket⁶.

Pocket Descriptors	Orthosteric site	Allosteric site (Without lipids)	Allosteric site (With lipids)
Druggability score (0-1)	0.9	0.008	0.9
Total SASA (\AA^2)	196.2	91.0	132.7
Polar SASA (\AA^2)	27.9	15.2	10.7
Apolar SASA (\AA^2)	168.3	75.8	121.9
Volume (\AA^3)	796.3	412.6	537.3
Mean local hydrophobic density	76.25	16.8	56.1

* SASA – Solvent-Accessible Surface Area

Table S4. Lipid compositions of the asymmetric bilayer used in the simulations. The fraction (%) of various lipids in the upper and lower leaflets are adopted from the published studies^{7, 8}.

Lipid type	Upper leaflet (%)	Lower leaflet (%)
POPC	39	15.7
Cholesterol	30.9	28.1
PSM	21.4	9.1
POPE	8.7	26.4
POPI	0	10.7
POPS	0	10

Table S5. The total, nonpolar, and polar buried surface area (BSA) and membrane-exposed surface area (MESA) of ORG27569 and its analogs when they are bound to the CB1R allosteric site.⁹

Ligand	SASA (Å ²)			Nonpolar SASA (Å ²)			Polar SASA (Å ²)		
	Total	BSA (%)	MESA (%)	Total	BSA (%)	MESA (%)	Total	BSA	MESA
ORG27569	703	379 (53.9)	324 (46.0)	646	330 (51.0)	317 (49.0)	56.3	49 (81.0)	7 (12.4)
Compound 21	677	331 (49.0)	345 (51.0)	617	300 (48.6)	317 (51.4)	59.5	31 (52.6)	28 (47.4)
ICAM-b	772	332 (43.0)	440 (57.0)	716	296 (41.3)	420 (58.7)	55.7	36 (64.3)	20 (35.7)
Compound 13	658	426 (64.8)	232 (35.2)	600	380 (63.2)	221 (36.8)	57.7	46 (79.7)	11 (20.3)
Compound 11j	741	462 (62.3)	279 (37.7)	694	421 (60.6)	273 (39.4)	47.1	41 (87.7)	6 (12.3)
Compound 12f	760	353 (46.4)	407 (53.6)	709	324 (45.7)	385 (54.3)	51.3	29 (56.7)	22 (43.3)

Table S6. The binding free energies of various CB1R ligands were calculated using the MMPBSA method considering explicit membrane lipids (See the Methods section for details).

Ligand	The free-energy contribution by individual binding site residues(kcal/mol)											Binding free energy(kcal/mol)
	L138	I141	L142	G157	S158	V161	V234	F237	C238	W241	I245	
ORG27569	-0.31	-0.26	-0.50	-0.60	-1.07	-0.96	-0.23	-1.11	-0.91	-2.42	-1.05	-46.83 ± 3.54
Compound 21	-0.02	0.03	0.02	-0.18	-0.62	-0.40	-0.84	-1.43	-1.15	-2.65	-1.15	-46.09 ± 2.58
ICAM-b	-0.02	0.00	0.00	-0.05	-0.40	-0.06	-1.01	-1.72	-1.92	-2.69	-1.18	-55.24 ± 3.22
Compound 13	-0.31	-0.77	-0.85	-0.23	-0.63	-0.91	-1.15	-1.18	-1.04	-0.84	-0.03	-41.71 ± 3.04
Compound 11j	-0.33	-0.55	-0.66	-0.84	-1.19	-1.23	-0.91	-1.49	-0.69	-2.14	-0.47	-51.42 ± 3.00
Compound 12f	-0.19	0.00	-0.01	0.21	-0.65	-1.91	-0.07	-0.15	-0.14	-2.79	-1.36	-53.61 ± 2.85

Table S7. The per-lipid binding free energy contribution by several lipids for various CB1R ligands, calculated using the MMPBSA method considering explicit membrane lipids (See the Methods section for details).

Upper/lower leaflet	The MM-PBSA binding free energy (kcal/mol)					
	ORG27569	ICAM-b	Compound 21	Compound 13	Compound 12f	Compound 11j
U1	-0.47 (POPC)	-1.84 (POPC)	-0.34 (CHOL)	-1.60 (POPC)	-0.48 (POPC)	-0.30 (POPC)
U2	-0.63 (CHOL)	-1.58 (POPC)	-0.41 (POPC)	-0.64 (PSM)	-0.41 (POPC)	-1.41 (PSM)
U3	-0.58 (POPC)	-0.36 (PSM)	-0.10 (POPC)	-0.79 (POPC)	-0.21 (POPC)	-1.32 (PSM)
L1	-4.77 (POPC)	-6.69 (POPE)	-3.76 (POPC)	-3.77 (CHOL)	-6.06 (POPC)	-4.54 (POPE)
L2	-1.66 (POPI)	-2.35 (POPE)	-3.45 (POPS)	-4.16 (POPS)	-2.92 (POPC)	-3.46 (POPI)
L3	-0.90 (POPS)	-1.21 (POPS)	-0.75 (POPC)	-1.03 (CHOL)	-0.28 (POPE)	-1.98 (POPS)
L4	-0.75 (CHOL)	-0.74 (CHOL)	-0.002 (CHOL)	-0.31 (POPI)	-0.43 (CHOL)	-0.75 (CHOL)

*Lipids that are within 4 Å from the ligands were included as part of the binding site for the MMPBSA calculations. Three such lipids with the highest energy contributions from the upper (U1, U2, and U3) and lower (L1, L2, and L3) leaflets are included in this table.

Table S8. The percentage contact occupancy (%) of the head and tail portions and alkyl chains of the studied ligands with various functional groups of the bilayer lipids.

ligand	K_B/EC_{50} (nM)	α	ligand part	Protein	Membrane			
					Cho	Pho	Gly	Alk
ORG27569	217.3	6.9	T	0.50	0.00	0.00	0.00	0.50
			A	0.55	0.00	0.00	0.06	0.40
			H	0.72	0.00	0.00	0.00	0.28
Compound 21	90*		T	0.47	0.00	0.00	0.00	0.53
			H	0.49	0.40	0.00	0.06	0.04
			No alkyl chain					
ICAM-b	469.9	17.6	T	0.52	0.00	0.00	0.05	0.43
			A	0.25	0.08	0.00	0.17	0.50
			H	0.64	0.00	0.00	0.00	0.36
Compound 13	207.4	19.7	T	0.22	0.00	0.00	0.00	0.78
			A	0.43	0.00	0.00	0.00	0.57
			H	0.52	0.00	0.00	0.01	0.46
Compound 11j	167.3	17.0	T	0.47	0.00	0.00	0.00	0.53
			A	0.48	0.00	0.00	0.03	0.48
			H	0.64	0.00	0.00	0.00	0.36
Compound 12f	89 .1	5.1	T	0.65	0.00	0.00	0.00	0.35
			A	0.22	0.04	0.00	0.03	0.71
			H	0.62	0.00	0.00	0.00	0.38

Table S9. The binding free energies of various CB1R ligands were calculated using the MMPBSA method, considering implicit heterogeneous membrane regions represented by distinct dielectric constants (See the Methods section for details).

Ligand	The free-energy contribution by individual binding site residues (kcal/mol)																Binding free energy (kcal/mol)	
	L138	I141	L142	L147	R148	H154	G157	S158	V161	L165	R230	V234	F237	C238	W241	T242		I245
ORG27569	-0.20	-0.37			-0.58	-0.88	-1.68	-1.53	-0.92		-1.05	-0.15	-1.51	-1.36	-3.53	-0.44	-1.10	-10.22 ± 0.3
Compound 21	0.00	0.00	0.00	0.02	-0.45	-0.76	-0.38	-1.00	-0.36	-0.74			-1.55		-3.67		-1.29	-8.50 ± 0.21
ICAM_b	0.01	-0.01	0.00	0.05	-0.41	-0.37	-0.21	-0.87	-0.06		-1.18	-1.16	-2.26	-2.93	-3.50	-0.60	-1.21	-8.88 ± 0.25
Compound 13	-0.20	-1.10	-1.01	-0.03	-1.01	-3.17	-0.81	-1.15	-0.98			-1.41	-1.46	-1.17	-1.39	-0.03	-0.06	-10.1 ± 0.24
Compound 11j	-0.39	-0.47	-0.65	0.21	-1.25	-1.48	-1.73	-1.35	-1.32	-0.37		-0.86	-1.74	-0.82	-3.70		-0.54	-12.7 ± 0.33
Compound 12f	-0.21	-0.05	-0.05		-0.66	-0.16	-0.05	-0.98	-1.94	-1.14	-0.51	-0.06	-0.21		-3.75		-1.53	-8.13 ± 0.26

Table S10. The amino acid details for the Cholesterol Consensus Motif (CCM) in GPCRs.

Position on TMHs	Typical CCM residue	Equivalent residue on CB1R
2.41	Phe, Tyr	His
4.39-4.43	Arg or Lys (at least one is required in any of these positions)	Arg at 4.39 Lys at 4.41
4.46	Ile, Val, Leu	Phe
4.50	Trp	Trp

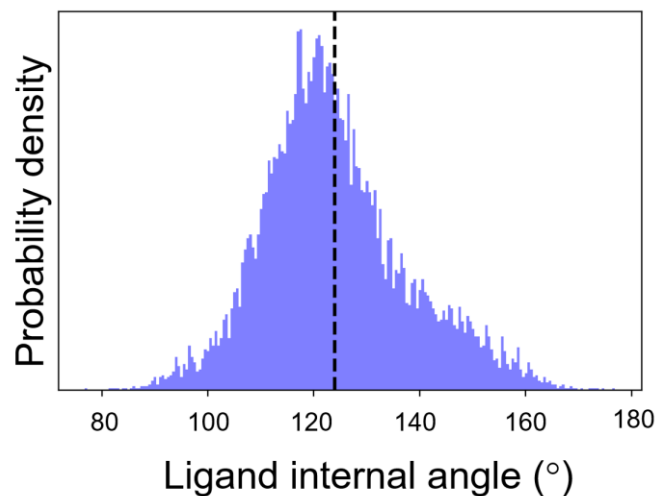


Fig. S1. The internal angle of ORG27569 within the lipid bilayer at and around its free energy minima ($Z_{\text{min}} \pm 2 \text{ \AA}$). The preferred conformation of ORG27569 in the bilayer was characterized by the internal angle calculated between two vertices formed by the head (indole ring) and tail (phenyl-piperidinyl ring) parts of the ligand using the amide nitrogen as the intersecting point (See Fig. 1 in the main text for the 2D structure of ORG27569).

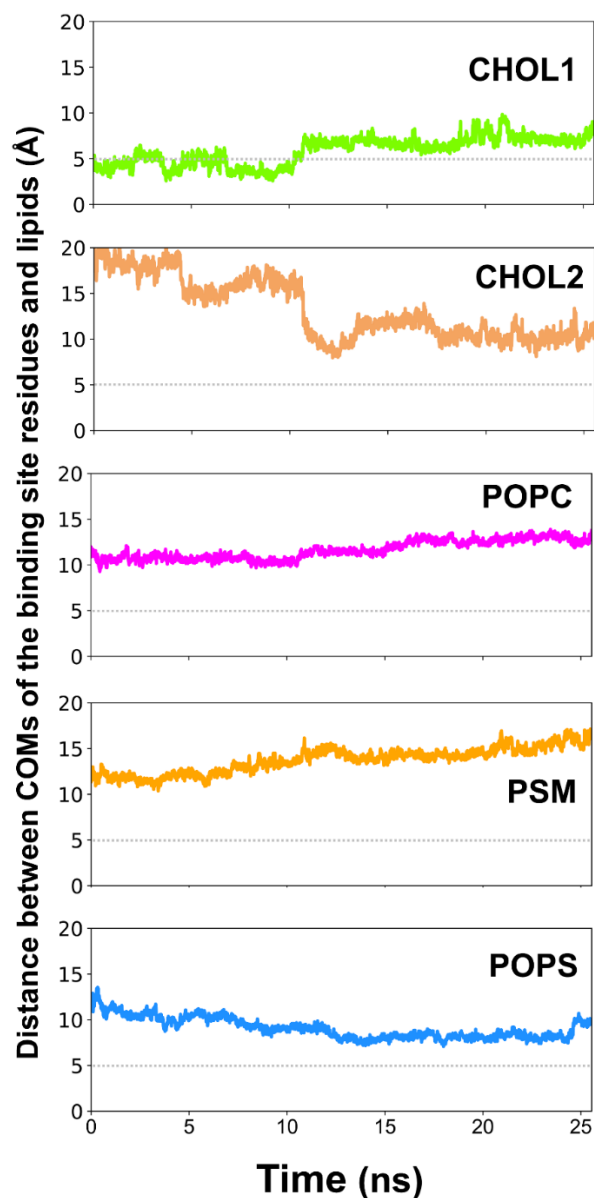


Fig. S2. Binding of ORG27569 during the WT-metaD simulation leads to the rearrangement of lipids around the binding site. (A) Rearrangement of lipids around the allosteric binding site caused by the ligand binding. The movement of lipids was evaluated by measuring the center-of-mass distance between the lipids and the binding site residues. Lipids shown include CHOL1 (green), CHOL2 (sandy brown), POPC (magenta), PSM (blue), POPS (orange).

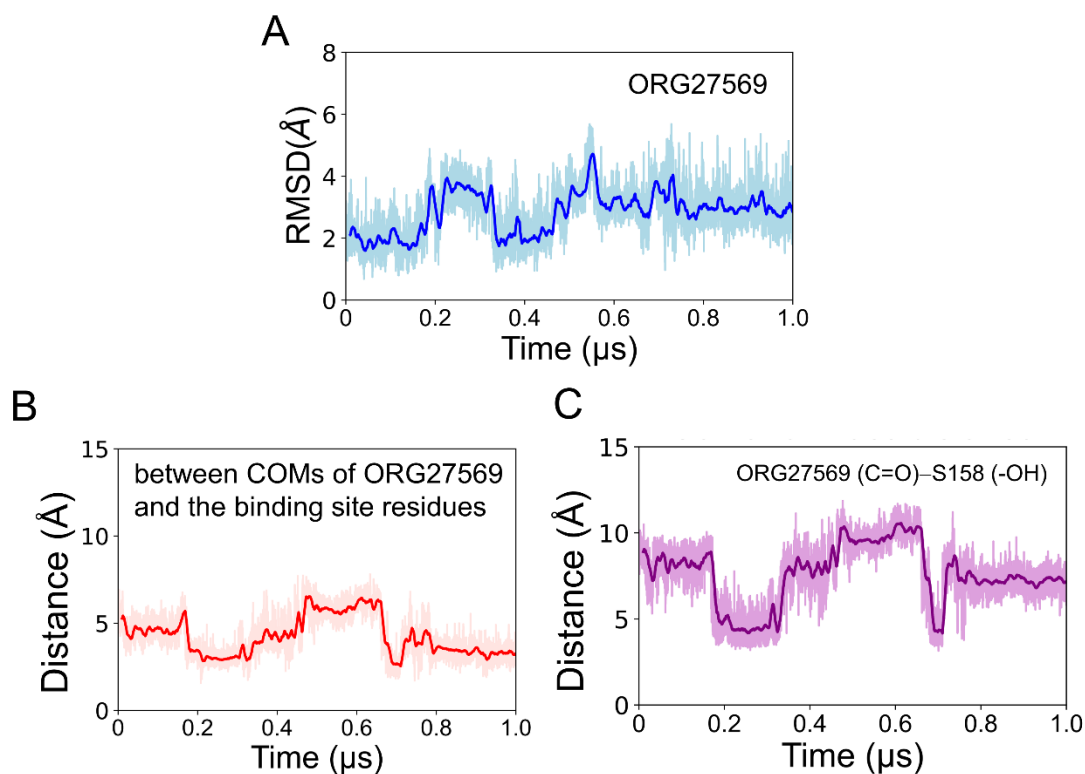


Fig. S3. ORG27569 remains stable at the binding site during the entire 1 microsecond long unbiased MD simulation. (A) The root-mean-square deviation (RMSD) of ORG27569 during the all-atom unbiased MD. The ligand undergoes a slight rearrangement between 200 - 400 ns, after which it assumes a stable conformation within the binding site for the rest of the simulation time. (B) The distance between the center-of-mass (COM) of the ligand and the binding site residues. (C) The distance between the carbonyl oxygen of ORG27569 and the oxygen atom of the sidechain -OH group of S158. This distance was used to track the orientation of the carbonyl oxygen atom on ORG27569, with larger distances indicating a flip towards the membrane lipids and vice versa.

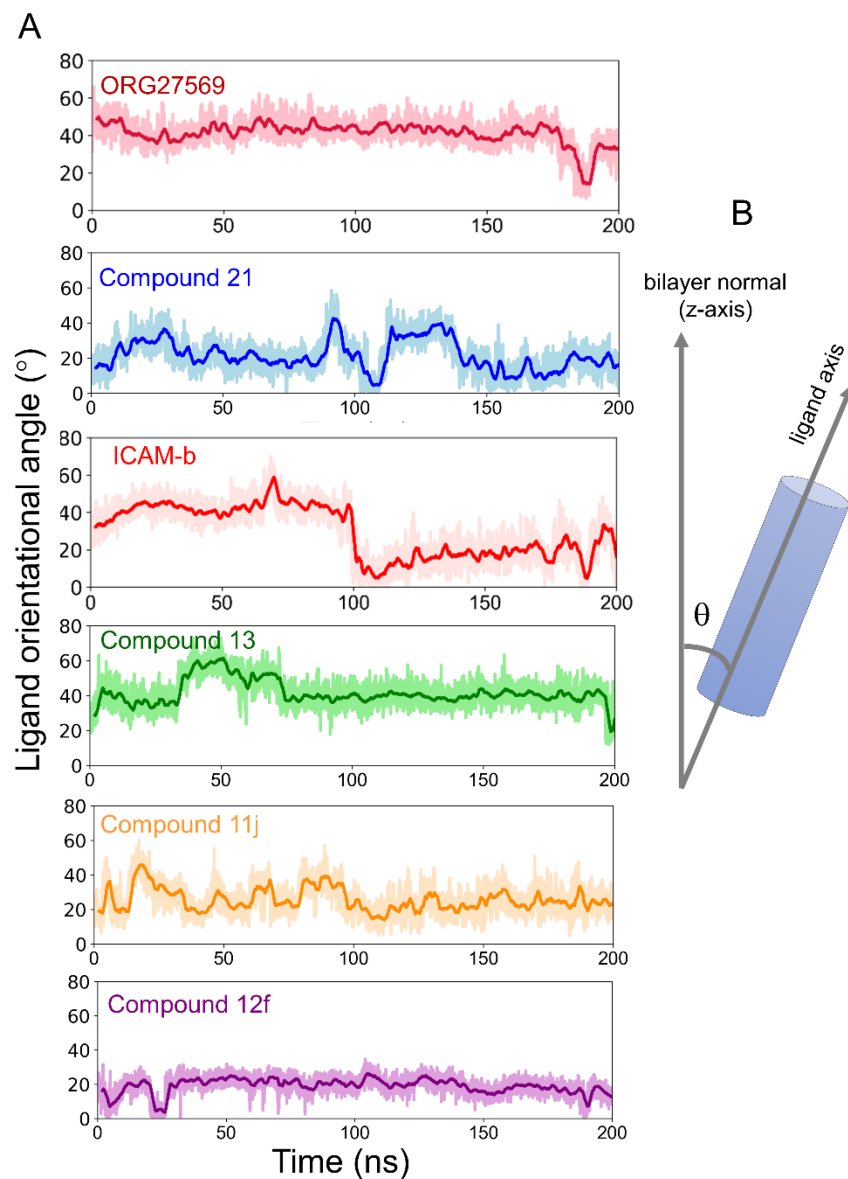


Fig. S4. The orientational angles of ORG27569 and its analogs at the allosteric site of CB1R. A) The orientational angle of each ligand through the entire simulation time was quantified as a tilt angle θ between the bilayer normal (z-axis) and the vector, connecting the two ends of the ligand (**B**). For each ligand, the chlorine atom at one end and the farthest aromatic carbon atom on the piperidine ring or the nitrogen of the dimethylamino group as the other end was considered as depicted in Fig. 8 of the main text.

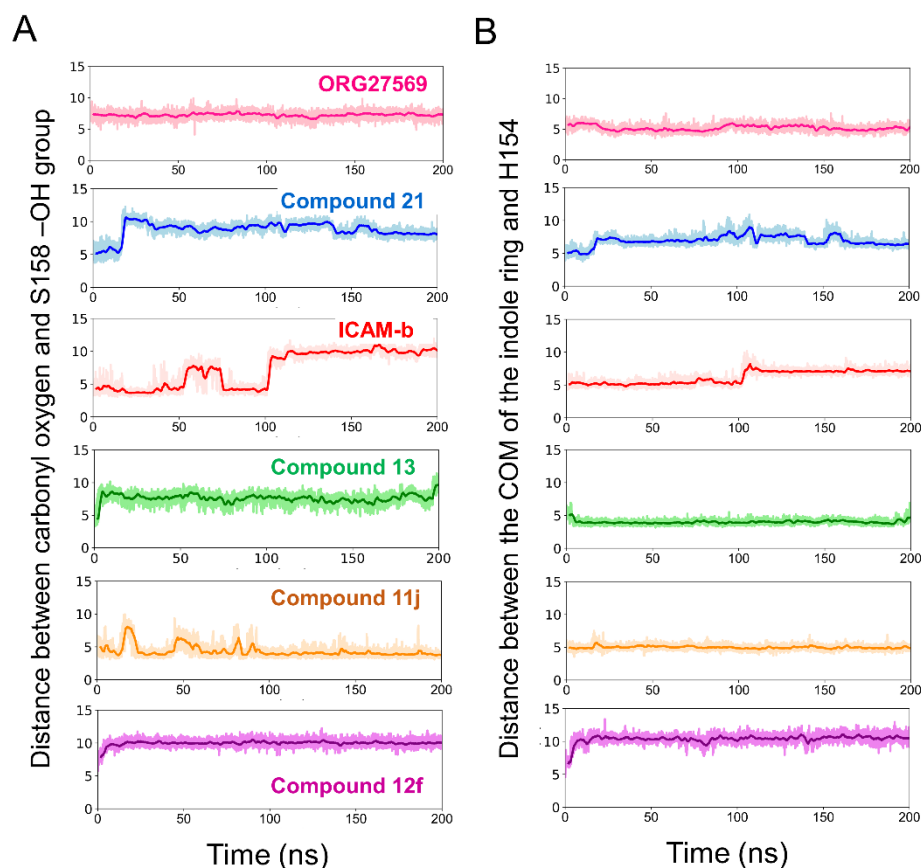


Fig. S5. The binding orientations of ORG7569 and analogs. A) Orientation of the ligands' carbonyl oxygen of the carboxamide group is shown as the distance between the carbonyl oxygen atom and the sidechain -OH group of S158. B) The depth of the analogs within the binding site is calculated as the distance between COMs of the indole ring and the imidazole ring of H154. Analogs shown include ORG27569 (pink), Compound 21 (blue), ICAM-b (red), Compound 13 (green), Compound 11j (orange), and Compound 12f (purple). For ORG27569, data from the last 200 ns of the 1- μ s long unbiased simulations were used.

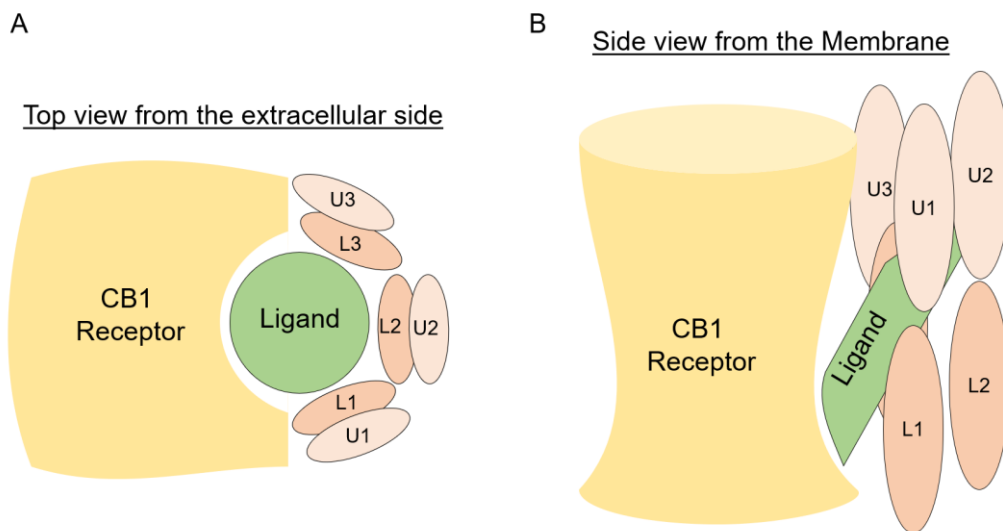


Fig. S6. Schematic representation of the CB1R-ligand complex in which the ligand is directly in contact with the membrane lipids. A-B) When bound at the CB1R transmembrane allosteric site, ORG27569 and analogs were significantly in contact with lipids from the lower (L1, L2, and L3) and upper (U1, U2, and U3) leaflets of the bilayer. Lipids within 4 Å distance from the ligand were included as part of the binding site in the MM-PBSA free energy calculations. The lipid-wise contributions toward the binding affinities are given in Table S7.

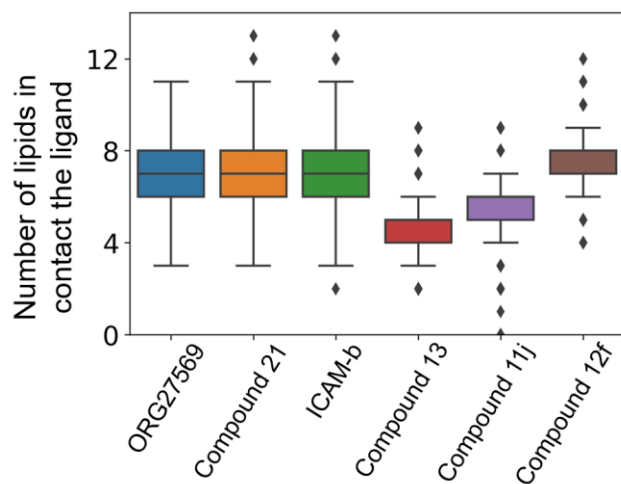


Fig. S7. The boxplot shows the number of lipid molecules directly in contact with the bound ligands at the transmembrane allosteric site of CB1R. The number of lipid molecules within 4 Å of the ligand was calculated through the entire simulation time (200 ns) for each frame of the simulation trajectory using the `gmx_select` command within the GROMACS suite.

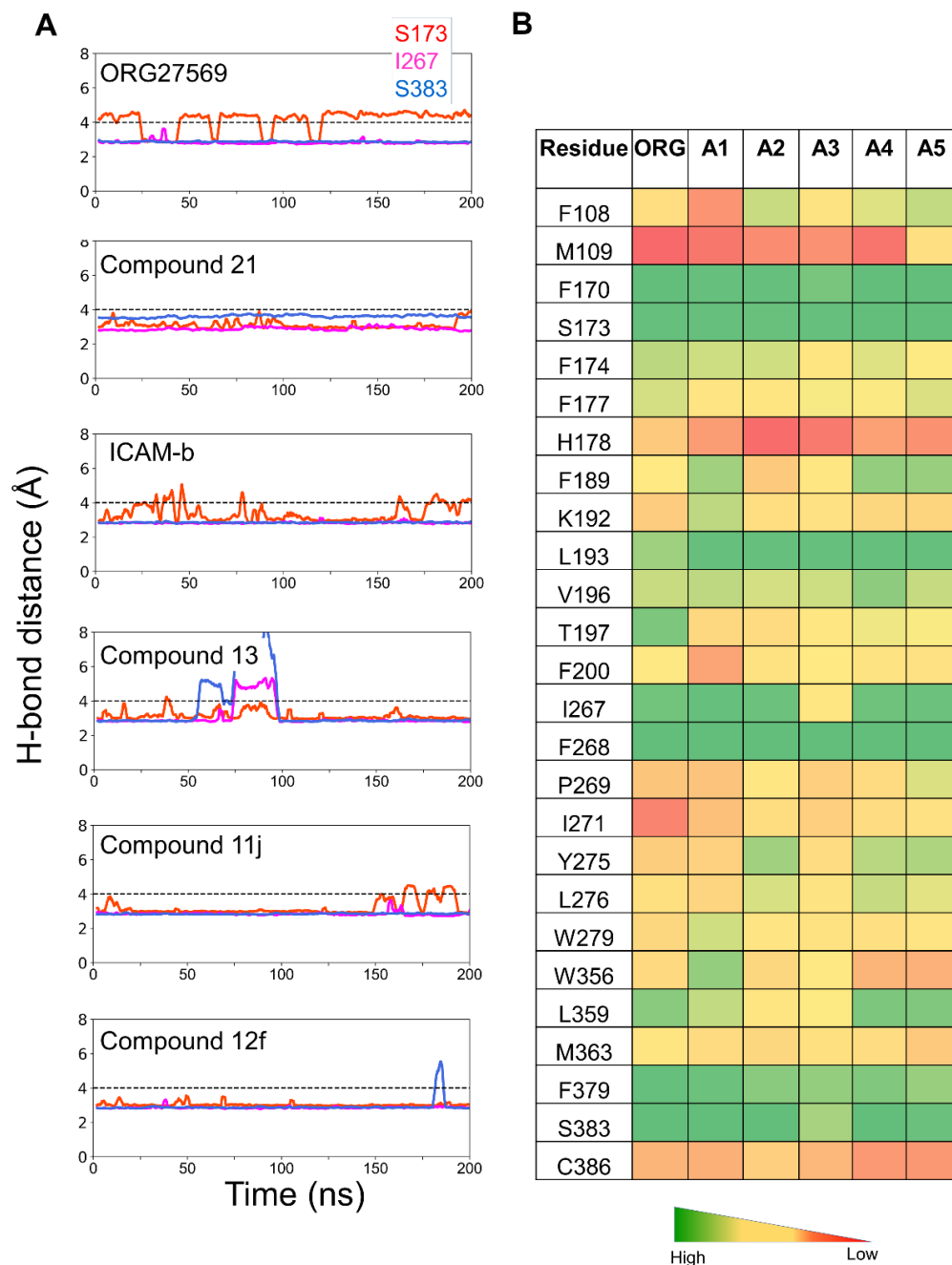


Fig. S8. The effect of ORG27569 and its various analogs on H-bond distances and other molecular interactions of the agonist, CC5940, at the orthosteric site. A) H-bond distances of CC5940 with the orthosteric binding site residues, S173 (orange), I267 (magenta), and S383 (royal blue). An arbitrary 4 Å distance is indicated in gray dotted lines. B) Heatmap showing the contact frequencies (% occupancy, the fraction of the simulation time during which the agonist is within 4 Å of a given residue) of CC5940 with various binding site residues, accounting for the effect of ORG27569 and its analogs on the agonist interactions. The following alphanumeric values are used to denote the compounds: ORG27569 – ORG, Compound 21 – A1, ICAM-b – A2, Compound 13 – A3, Compound 11j – A4, and Compound 12f – A5. Also, see Fig. 1 in the main text for the binding mode and molecular interactions of CC5940 with the orthosteric binding site residues.

A Residues that participate during the access and binding of ORG27569:
R186, N187, L190, I245, V249, L252, E258, and K259

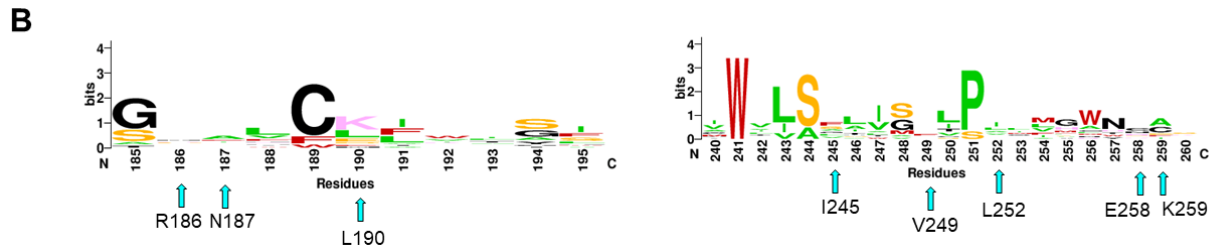
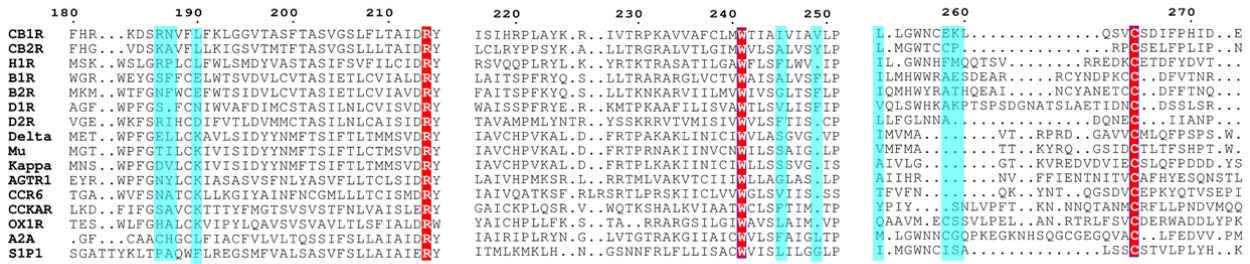


Fig. S9. Residues that were involved in the access process of ORG17569 to the transmembrane allosteric site of CB1 receptor. A) Multiple sequence alignment of several class A GPCRs, including CB1 and CB2 receptors. B) The logo maps created using the multiple sequence alignment reveal insignificant conservation of the residues among the receptors. CB1R – Cannabinoid 1 receptor; CB2R – Cannabinoid 2 receptor; H1R – Histamine 1 receptor; B1R – Beta 1 adrenergic receptor; B2R – Beta 2 adrenergic receptor; D1R – Dopamine 1 receptor; D2R – Dopamine 2 receptor; Delta – Delta opioid receptor; Mu – Mu opioid receptor; Kappa – Kappa opioid receptor; AGTR1 – Angiotensin II type 1 receptor; CCR6 - CC chemokine receptor 6; CCKAR - Cholecystokinin 1; OX1R – Orexin 1 receptor; A2A- Adenosine A2A receptor; SIP1 – Sphingosine 1 phosphate receptor.

A Allosteric binding site residues:
L132, I141, L142, H154, S158, V161, V234, F237, C238, W241, and I245

```

110      120      130      140      150      160      170      220      230      240      250
CB1R  ECF...MVLNPSQQLAIAVLSLTLTGFTVLENLIVLCVTL  LHSRLRCRPSYHFIGSLAVADLLGSVIFVYSFIDFHV.  (SIHRPLAYK.R...IVTRPKAVVAFCLMWTIAIVIAVLP
CB2R  KDY...MILSGPQKTAVAVLCTLLGLLSAENVAVLYLT  LSSHQLRRKPSYHFIGSLAGADFLASVVFACSFVNFHV.  (CLRYPPSYK.A...LLTRGRALVTLGIMVLSLAVSYLP
H1R   GNK...TMMASFPQLMPLVVLSTICLVTVGNLIVLYAV  RSEKRLH.TVGNLYIVLSVADLVIGAVVMPNLIYLL.  (SVQQPLRYL.K...YRTKTRASATILGAVFLSFLWV.IP
B1R   ESP...EPLSQOWTAGMGLMLALIVLLIVAGNVIVAI  AKTPELO.TLTNIFIMELASADLVMGLLVVPFGATIVV.  (AITSPPRYQ.S...LLTRARAGLIVTVAISLVSFLP
B2R   DVT...QERDEVWVVGMGIVMSLIVLAIIVGNTVITAE  AKFERLO.TVTNFIITSLACADLVMLGLAVVPPGAAHIL.  (AITSPPKYQ.S...LLTKNKARVILIMVIVISGLTSFLP
D1R   GLV...VERDFSVRILTACFLSLLILSTLIGNITVCAAV  IRFRHLRSKVTNFVIVSLAVSCLLVAVLVMPKVAVEI.  (AISSPFRYE.R...KMTPKAAFILISVATLSVLISFIP
D2R   GSD...GKADRPHYNYATLLTLLIAVIVFGNVIVCMVA  SREKALO.TTTNVLIVSLAVDLVATLVMPVWVYLEV.  (AVAMPMLYNTR...YSSKRRVTVMISIVVLSFTIS.CP
Delta PGA...RSASSLALAIATALYSAVCAVGLIGNIVMFGI  VRYTKMK.TATNIYIFNLAIADALATS.TLPPQSAYL.  (AVCHPVKAL.D...FRTPAKAKLINICIVWLASGVG.VP
Mu     P...TGSPSMITAITIMALYSIVCVVGLIGNIVMYVI  VRYTKMK.TATNIYIFNLAIADALATS.TLPPQSAYL.  (AVCHPVKAL.D...FRTPRNAKIINVCWLLSAGI.LP
Kappa . . .E.PAHISPAIPVITAVYSVVFVGLIGNIVMFI  VRYTKMK.TATNIYIFNLAIADALVTT.TMPFQSTVYL.  (AVCHPVKAL.D...FRTPKAKIINICIVWLLSAGV.IS
AGTR1 K... . . .AGRHNYIFVMIPTLYSIIFVVGIFIGNIVVIT  YFYMKLK.TVASVFLNLAIAACILFLL.TLPLWAVYTAM  (AIVHPMKSR.L...RRTMLVAKVTCIIVWLLAGLAS.LP
CCR6  L... . . .QEVRFQSRFLVPIAYSLLICVFGLLIGNIVVIT  AFYKKAR.SMTDVYLLNMAIACILFVL.TLPPWAVSHA.  (AIVQATKSF.RLRSRTLFRSKIICLVVWGLSIVIS.SS
CCKAR DQP...RPSKEWQAPVQILLYSLIFLLSVLIGNITVITV  IRNKMR.TVTNIFLLSLAVSCLMLCLFCMPFNLIPLN.  (AICKPLQSR.V...WQTKSHALKVIAATVCLSTTIM.TF
OX1R  WRDYLYPKQYEW...VLIAAYVAVFVVALIGNITVCLAV  WRNHHMR.TVTNIFVNLSLAVLVTAIICLPASLLVDI.  (AICHPLLEK.S...TA...RRAKSLIGVAVSIAIM.VF
A2A   GSS...V... . . .YI...T.VELAIAVLAIIGNIVCMVA  WLNENLG.NVTNIFVSLAAADLVAVGLAIPFAITIST.  (AIRIPLRYN.G...LVTGTRAKGIITAIQVLSFAIGLTP
S1P1  LNI...SADKENSIKLTSVVFILICCFIIPENIFVLLT  WTKKPH.RFMYHFIGSLASCLLAGVAYTAN...LLL.  (ITMLKMLH...N...GNNFRIFLLISAGWISLILGLLP

```

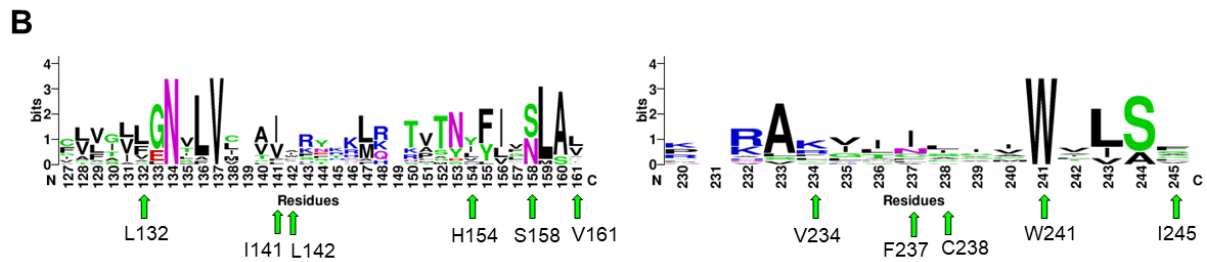


Fig. S10. Critical residues at the transmembrane allosteric binding site of CB1 receptor.
A) Multiple sequence alignment of several class A GPCRs, including CB1 and CB2 receptors.
B) The logo maps created using the multiple sequence alignment reveal that only a few residues have moderate to significant conservation among the receptors.

Compound 21

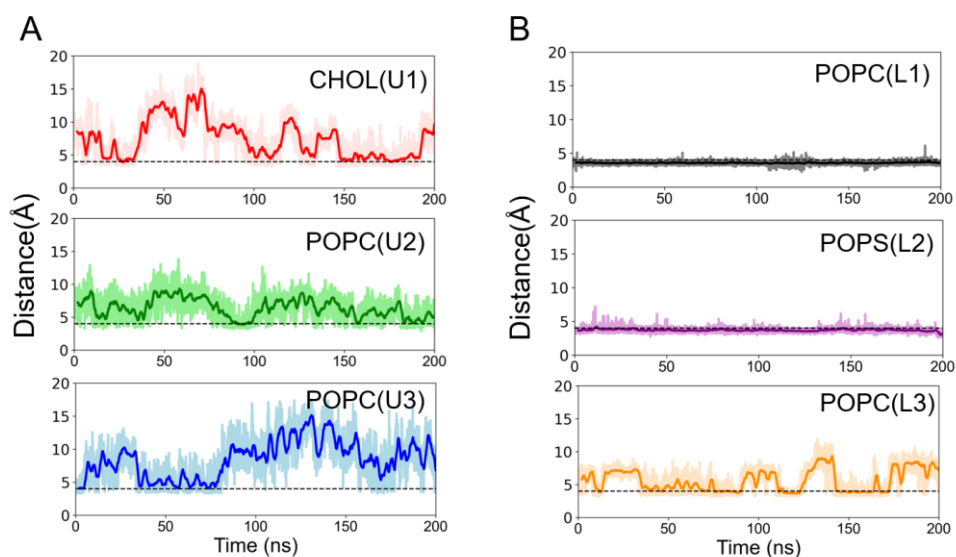


Fig. S11. Lipid species that were directly in contact with Compound 21 when it was bound at the CB1R transmembrane allosteric site. The distances between Compound 21 and the center-of-mass of various lipid species from the upper and lower leaflets are given in A and B, respectively. The distances were monitored through the 200 ns simulation time.

ICAM-b

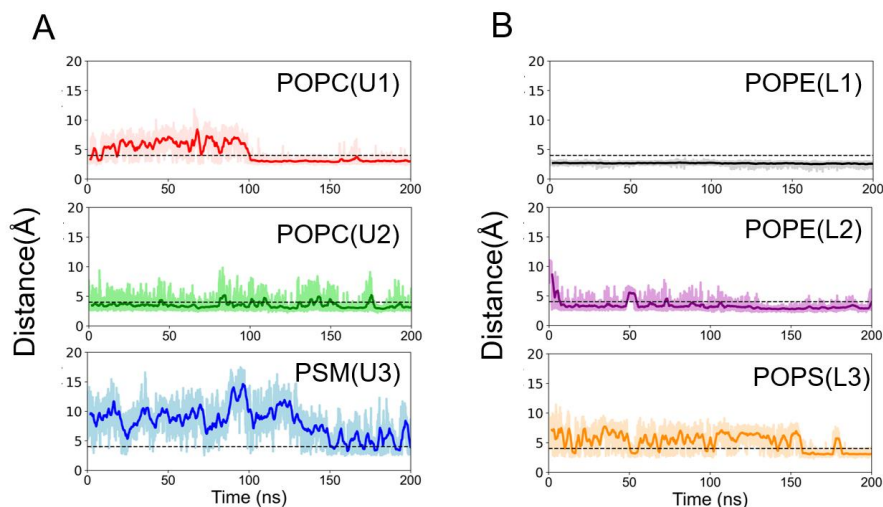


Fig. S12. Lipid species that were directly in contact with ICAM-b when it was bound at the CB1R transmembrane allosteric site. The distances between ICAM-b and the center-of-mass of various lipid species from the upper and lower leaflets are given in A and B, respectively. The distances were monitored through the 200 ns simulation time.

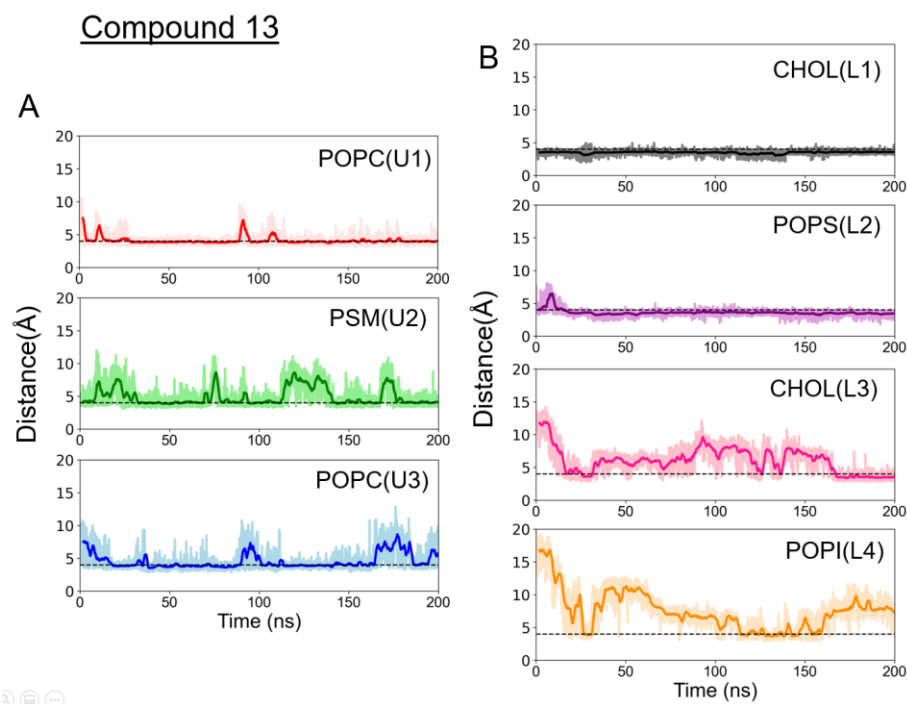


Fig. S13. Lipid species that were directly in contact with **Compound 13** when the ligand was bound at the **CB1R** transmembrane allosteric site. The distances between Compound 13 and the center-of-mass of various lipid species from the upper and lower leaflets are given in A and B, respectively. The distances were monitored through the 200 ns simulation time.

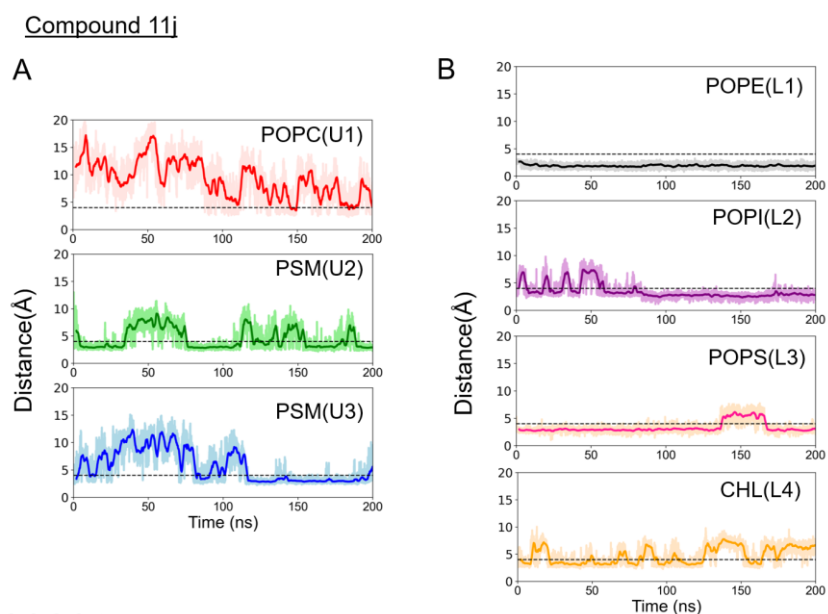


Fig. S14. Lipid species that were directly in contact with **Compound 11j** when it was bound at the **CB1R** transmembrane allosteric site. The distances between Compound 11j

and the center-of-mass of various lipid species from the upper and lower leaflets are given in A and B, respectively. The distances were monitored through the 200 ns simulation time.

Compound 12f

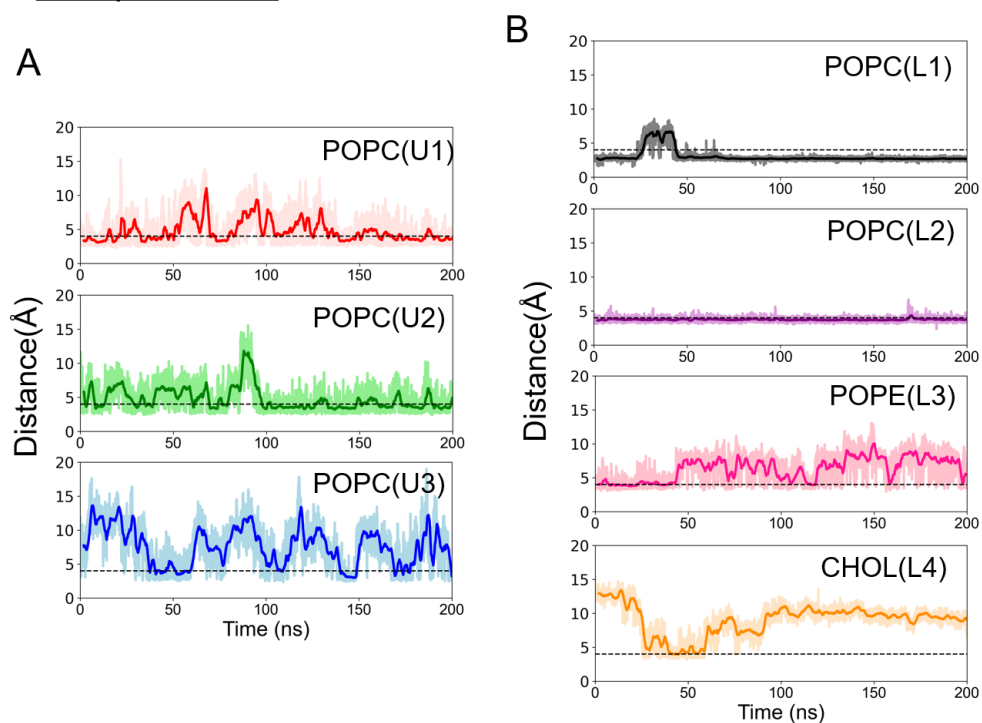


Fig. S15. Lipid species that were directly in contact with Compound 12f when it was bound at the CB1R transmembrane allosteric site. The distances between Compound 12f and the center-of-mass of various lipid species from the upper and lower leaflets are given in A and B, respectively. The distances were monitored through the 200 ns simulation time.

References:

1. Bio-Loom, B.-. BioByte Corp, 212 E Rowland St, DPT# 55021, Covina, CA 91723. **2021**.
2. Ahn, K. H.; Mahmoud, M. M.; Samala, S.; Lu, D.; Kendall, D. A. Profiling two indole-2-carboxamides for allosteric modulation of the CB1 receptor. *J Neurochem* **2013**, 124, 584-589.
3. Mahmoud, M. M.; Ali, H. I.; Ahn, K. H.; Damaraju, A.; Samala, S.; Pulipati, V. K.; Kolluru, S.; Kendall, D. A.; Lu, D. Structure-activity relationship study of indole-2-carboxamides identifies a potent allosteric modulator for the cannabinoid receptor 1 (CB1). *J Med Chem* **2013**, 56, 7965-7975.
4. Khurana, L.; Ali, H. I.; Olszewska, T.; Ahn, K. H.; Damaraju, A.; Kendall, D. A.; Lu, D. Optimization of Chemical Functionalities of Indole-2-carboxamides To Improve Allosteric Parameters for the Cannabinoid Receptor 1 (CB1). *J Med Chem* **2014**, 57, 3040-3052.
5. Piscitelli, F.; Ligresti, A.; La Regina, G.; Coluccia, A.; Morera, L.; Allarà, M.; Novellino, E.; Di Marzo, V.; Silvestri, R. Indole-2-carboxamides as allosteric modulators of the cannabinoid CB₁ receptor. *J Med Chem* **2012**, 55, 5627-31.
6. Le Guilloux, V.; Schmidtke, P.; Tuffery, P. Fpocket: An open-source platform for ligand pocket detection. *BMC Bioinformatics* **2009**, 10, 168.
7. Ingólfsson, H. I.; Melo, M. N.; van Eerden, F. J.; Arnarez, C.; Lopez, C. A.; Wassenaar, T. A.; Periole, X.; de Vries, A. H.; Tieleman, D. P.; Marrink, S. J. Lipid Organization of the Plasma Membrane. *Journal of the American Chemical Society* **2014**, 136, 14554-14559.
8. Van Meer, G.; Voelker, D. R.; Feigenson, G. W. Membrane lipids: where they are and how they behave. *Nat. Rev. Mol. Cell Biol* **2008**, 9, 112-124.
9. Szlenk, C. T.; Gc, J. B.; Natesan, S., Does the lipid bilayer orchestrate access and binding of ligands to transmembrane orthosteric/allosteric sites of G protein-coupled receptors? *Mol Pharmacol* **2019**, 96 (5), 527.